Effect of Propane-Methanol Blending Ratio on the Stretched and Unstretched Flame Speeds at Elevated Initial Temperatures

Ahmed AA. Abdulraheem
Ph. D. student
Mechanical Engineering Department
University of Technology
Iraq

Adel M. Saleh
Assistant Professor
Mechanical Engineering Department
University of Technology
Iraq

Haroun AK Shahad
Professor
Mechanical Engineering Department
University of Babylon
Iraq

The unstretched flame speed of the premixed propane-methanol/ air flames has been studied experimentally in a constant volume combustion chamber with central ignition. The experiments were done at atmospheric pressure and stoichiometric air/fuel ratio. Various blending ratios of methanol (0%, 20%, 40%, 60%, 80%, 100%) by volume, and different elevated initial temperatures (348 K, 373 K, and 398 K) were used in this study. In general, the results indicated that the unstretched flame speed increased with increasing both methanol blending ratio and initial temperature. For M60 the increment value of unstretched flame speed at T_i=398K was about 9% compared with that of pure propane and by elevating the initial temperature for the same blend ratio (M60) from 348 K to 398 K the increment value was about 8.8%. It is also noticed that Markstein length decreased with increasing both initial temperature and blending ratio, which is indicate that flame instability increased with increasing these parameters.

***Keywords**: Blending, Constant volume chamber, Initial temperature, Markstein length, Un-stretched flame speed*

1. INTRODUCTION

Increasing the concern of fossil fuels depleting and air pollution lead to that improving engine fuel economy and reducing exhaust emissions had become the major topics in combustion researches and engines manu–facture [1-7]. Many studies focused to search for alternative fuels in addition to enhance the combustion process since the 1970s [8]. Some of the alternative fuels reported in the literature which are used for spark ignition engines were alcohols, compressed natural gas (CNG), hydrogen, liquid petroleum gas (LPG), dimethyl ether (DME), and others that used in various internal combustion engines [9].

Methanol is considered as one of the important alternative fuels due to its advantages of environmental friendly, can be prepared from multiple sources, and having high octane number compared with that of fossil fuels [10], However, it also has some problems due to its low energy density and high latent heat of vaporization. It is reported that methanol fuel having a high specific fuel consumption when used in internal combustion engines compared with conventional fuels such as gasoline or diesel fuels [10]. Therefore, methanol is widely used as an additive into other fuels. In addition to that recent increased the use of propane as a fuel in transport vehicles [11] led the propane to be a key fuel candidate of study.

Laminar flame speed is a necessary parameter describing the physical and chemical properties in propagation of flame, and to validate the chemical kinetic model. It is essential for studying turbulent flame [12]. Constant Volume Chamber (CVC) method is one of several methods used in the field of flame speed, which is broadly applied as one of the non-sta–tionary methods to measure burning velocity (S_u) and flame speed (S_l) with reliable experimental results [13]. This method can be applied at a wide range of initial pressure (0.1 – 60 bar) compared with other methods [14]. Several factors influence on the accuracy of experiments in the CVC method, including the effect of spark ignition, chamber confinement, radiation heat loss, flame stretch, and flame instability [11,13,14]. To get precise measurements of laminar flame speed, the effect of the above-mentioned factors should be accurately minimized.

The internal cavity of the CVC can be designed with cylindrical or spherical shapes at different dimensions. Salih and Chaichan, [17] conducted their experiments in a cylindrical chamber with a length and inner diameter of 305 mm. Galmiche et al. [18] used a cylindrical vessel made from stainless steel with 24.32 L inner volume. Hinton and Stone [19] utilized 160 mm inner diameter of spherical vessel, while Mannaa et al. [20] used a spherical stainless steel combustion chamber with inner diameter of 330 mm. Other study conducted by Yasiry and Shahad [21] with 190 mm inner diameter and 250 mm length cylindrical vessel. Cylindrical cavity with an inner diameter of 80 mm and a length of 268 mm used by Yao et al. [22]. Bao et al. [23] carried out their experiments in a spherical vessel with 350 mm inner diameter. Lhuilier et al. [24] done their experiments in a spherical stainless steel combustion chamber with a volume of 4.2l. Linteris and Babushok

Received: July 2021, Accepted: December 2021
Correspondence to: Ahmed AA. Abdulraheem
Ph. D. student in Mechanical Engineering Department
University of Technology, Bghdad, Iraq
E-mail: 21977@student.uotechnology.edu.iq
doi: 10.5937/fme2201121A

[25] used a spherical vessel with volume of 3.05 L. A stainless-steel cylindrical combustion chamber with an internal diameter and length of 305 mm utilized by Duva et al. [26].

Flame stretch is a quantity which measures the stretch amount of the surface of flame due to the cur–vature and the outer velocity field strain. it is required to studying the effect of the stretch on the burning ve–locity. The rate of flame stretch is $K = 2S_n/r_f$ for the spherical propagation flame. The un-stretched flame speed (S_l) and Markstein length of burned gas, (L_b) can be determined by extrapolate the S_n to zero stretches.

Initial temperature considered as the most significant factor influencing flame speed and burning velocity with direct proportional relation. It allows a more stable flame propagation. The following equation is the most common correlation expressing the effect of initial pressure (P_i) and temperature (T_i):

$$S_u = S_{u,o}\left(\frac{T_i}{i,o}\right)^{\gamma}\left(\frac{P_i}{P_{i,o}}\right)^{\beta} \quad (1)$$

where (o) represent the reference conditions ($T_{i,o}$ = 298 K, $P_{i,o}$ = 1 bar). The exponent power for pressure and temperature (β, and □) were discussed broadly by Konnov et al. [27]. It differs as a function of several factors such as: equivalence ratio, fuel type, and the oxidizer. Varghese and Kumar [28] examined laminar flame speed for mixtures of $H_2/CH_4/CO_2/CO/N_2$/air at high initial pressures and temperatures. They suggested a power-law correlation, as shown below:

$$S_u = S_{u,o}\left(\frac{T_i}{i,o}\right)^{\alpha_o+\alpha_1\left(1-\frac{P_i}{P_{i,o}}\right)}\left(\frac{P_i}{P_{i,o}}\right)^{\beta_o+\beta_1\left(1-\frac{T_i}{T_{i,o}}\right)} \quad (2)$$

Han et al. [29] investigated the S_u for natural gas at an initial pressure of two bars under different initial temperatures. They showed that laminar flame speed increased with increasing the temperature for all mix–tures examined.

Many researchers investigate S_u ad S_l for methanol blending fuels. Metghalchi and Keck [30] proposed empirical equations for S_u of the mixtures of methanol, indolene and isooctane at different initial temperatures and pressures. Beeckmann et al. [31] and Zhang et al. [32] studied the laminar flame speed of methanol-iso–octane blends at different initial temperatures and atmos–pheric pressure. They found that the blends have S_u va–lues higher than isooctane but lower than met–hanol. Liu et al. [33] investigated laminar flame speed for hydrogen-methanol blends, and suggested correlation for it.

According to the literature review, there are a few studies reported data for the blends of methanol and propane. Therefore, the aim of this study is to investigate the effect of methanol-propane blending ratios and the effect of initial temperature (that have not been used in other previous studies) on the unstretched flame speed and Markstein length in a cylindrical constant volume combustion chamber (CVCC) using schlieren technique. The study was conducted under atmospheric pressure and at stoichiometric ratio, for different initial temperatures (348 K, 373 K, and 398 K) and various blending ratios:

- 0% methanol-100% propane (M0)
- 20% methanol-80% propane (M20)
- 40% methanol-60% propane (M40)
- 60% methanol-40% propane (M60)
- 80% methanol-20% propane (M80)
- 100% methanol-0% propane (M100)

2. EXPERIMENTAL SETUP

In this study, the Constant Volume Combustion Chamber (CVCC) method and schlieren photography technique are used to measure the flame speed. The complete setup of the rig and the schematic layout are shown in figures (1) and (2), respectively. The parts of the rig are fabricated and assembled in the laboratories of Mechanical Engineering Department at the University of Technology / IRAQ.

The combustion chamber is built from a stainless-steel type 316 cylinder with 305 mm inner diameter, and 400 mm length with a volume of 29 L. Two pressure resisting high transparency windows with 120 mm net diameter and thickness of 20 mm are fixed on the opposite sides of the cylinder to allow the optical access for combustion process. Seven sockets are welded to the cylinder, two of them placed at opposed, co-linear position used to insert and fixed two spark ignition electrodes, which are connected to the ignition system. The others used for liquid fuel injection, admitting gaseous fuel and air, exhaust gases, and inserting thermocouple type PT-100, and pressure transmitter. A robust stainless-steel stand was used to hold the combustion chamber.

The fuel injection unit, (figure 3) is used to induct the gaseous fuel (propane)/air mixture into the com–bustion chamber, while the liquid fuel (methanol) was injected directly to the combustion chamber using liquid fuel injection valve. An electrical control board unit is fabricated and utilized to facilitate and regulate conducting the experiments accurately. The unit supplies 12 V DC to the solenoid valves and regulates and controls the voltage entering to the ignition burner transformer.An electronic circuit unit is constructed to supply the required powerful spark to the electrodes and to control its timing. A schlieren technique was used to visualize the process of flame propagation with a high-speed camera (AOS -Q PRI) using a light source and plano-convex lenses as shown in figure (4).

The thermocouple and the pressure transmitter were calibrated regularly over different temperature and pressure ranges at the Central Organization for Standardization and Quality Control (COSQC) of Iraq.

3. TEST PROCEDURE

The first step started with vacuum process to scavenge the combustion chamber from any previous gases until its pressure reaches approximately -0.94 bar, then flushing process takes place by injecting air inside the combustion chamber for 3-4 minutes. This step is repeated twice to ensure that the combustion chamber is flushed completely from previous test. The vacuum

process is repeated for the three times to prepare the CC for injecting fuels and air according to the mixing ratio which was calculated previously. After that, turning on the heating system to heat up the combustion chamber to the desired temperature. In the next step, propane fuel is injected to the combustion chamber by fuel injection unit, while methanol fuel is injected by the liquid fuel injection valve according to its partial pressure. The mixing process is based on Gibbs-Dalton law of partial pressures for each mixture component. Subsequently, the air is admitted to the combustion chamber until reaches the required total pressure. The mixture is left for 5-6 minutes to ensure perfect mixing before igniting the mixture. The spark duration is set at 10 ms. Then the ignition switch and the camera trigger with 600×600 pixels, 3536 fps are pushed simultaneously to initiate recording and combustion processes. The results are recorded for each condition. In addition, the photographs of flame propagation are taken and then analysed using Tracker 5.1.5 software.

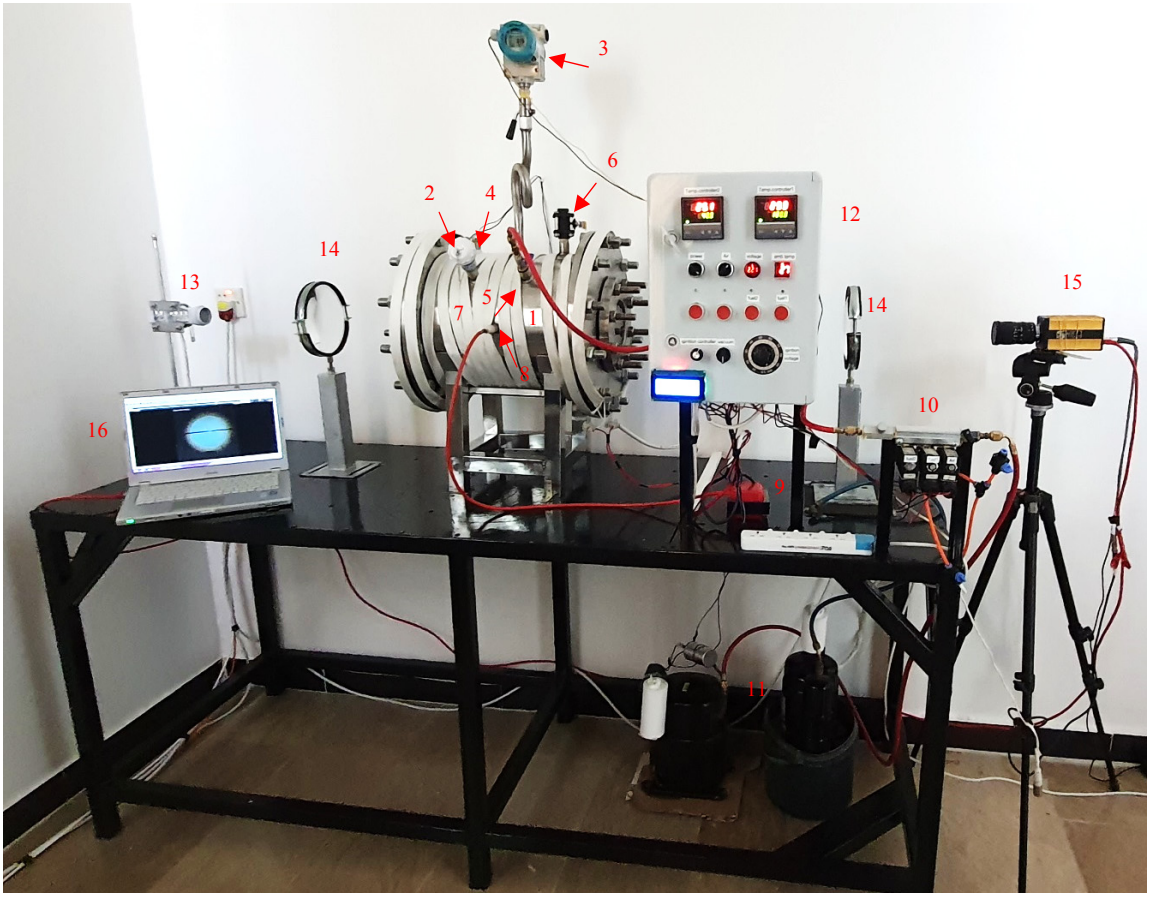

Figure 1. Photograph of the experimental apparatus used in the study. (1) Combustion chamber, (2) Thermocouple, (3) Pressure transmitter, (4) Liquid fuel injection valve, (5) Inlet valve, (6) Exhaust valve, (7) Electrical heating tape, (8) Sparking ignition electrodes, (9) Ignition burner transformer, (10) Injection unit, (11) Vacuum pump, (12) Electrical control board unit, (13) Light Source, (14) Two lenses (15) High-speed camera, and (16) PC computer.

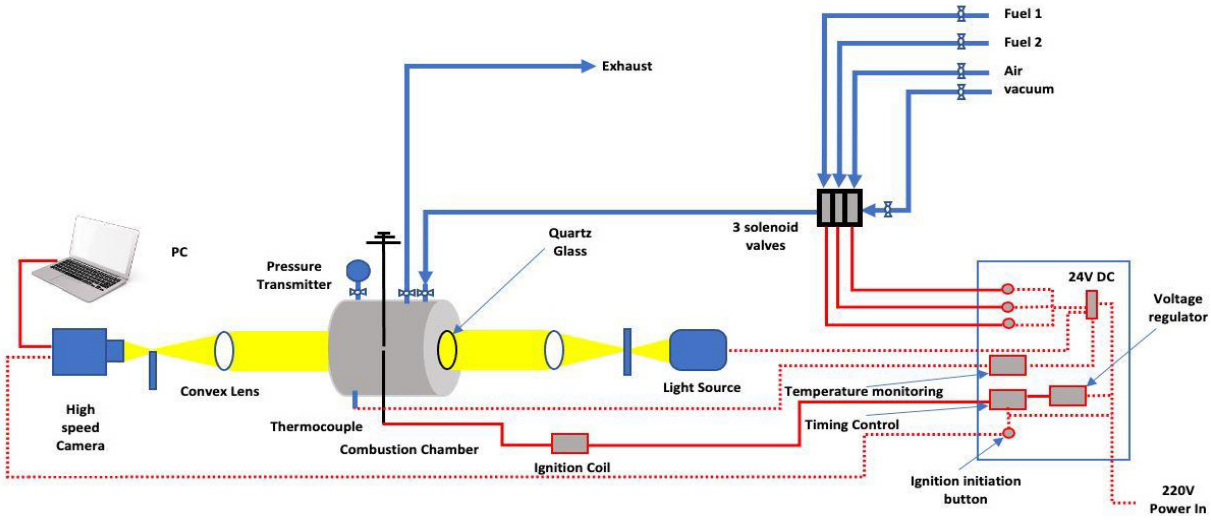

Figure 2. Schematic diagram of the experimental set up.

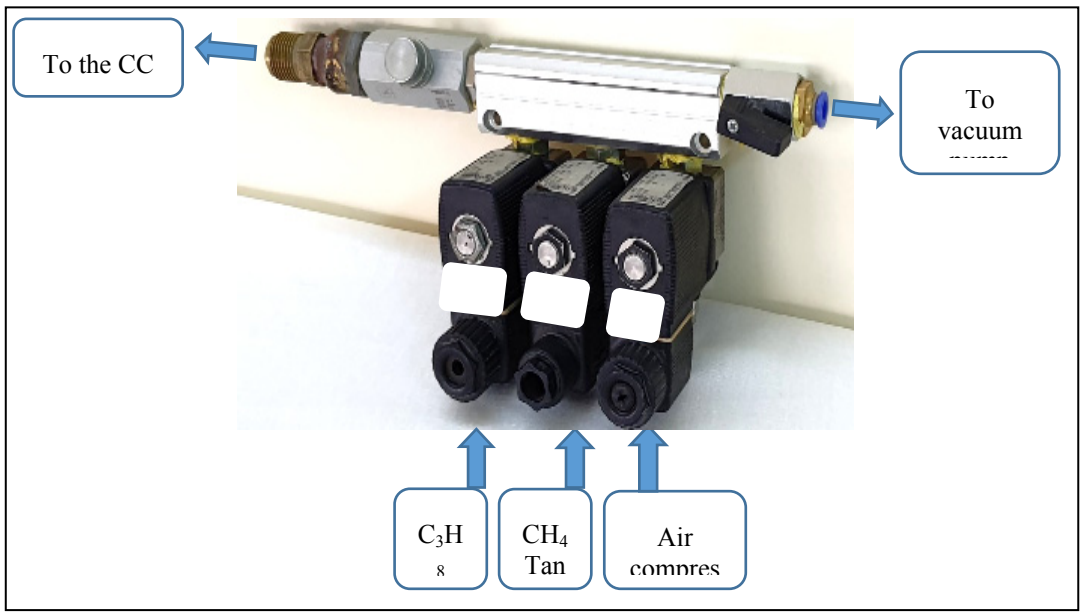

Figure 3. Fuel injection unit

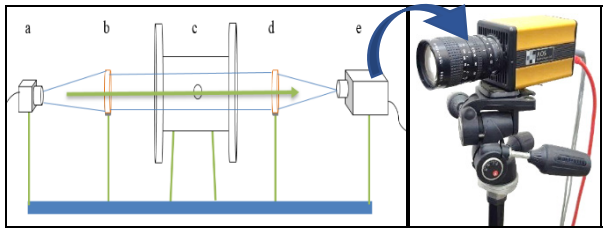

Figure 4. Schematic diagram for capturing unit a) illumi–nator, b) collimating lens, c) combustion chamber, d) de-collimating lens and e) high speed camera.

To test the accuracy of our system, the laminar burning velocity (S_u) for methane/air mixture at 1bar and ambient temperature for different equivalence ratios are compared with results of other researchers as shown in figure (5). Also, repeatability tests are carried out by repeated the experimental test for five times using the same fuel type (methane) and the same conditions (equivalence ratio, initial temperature, and initial pressure). Figure (6) shows that the results of repeatability are reasonable, since all the curves obtained have the same trend and the maximum percentage error at a radius of 2cm was 5.3 %.

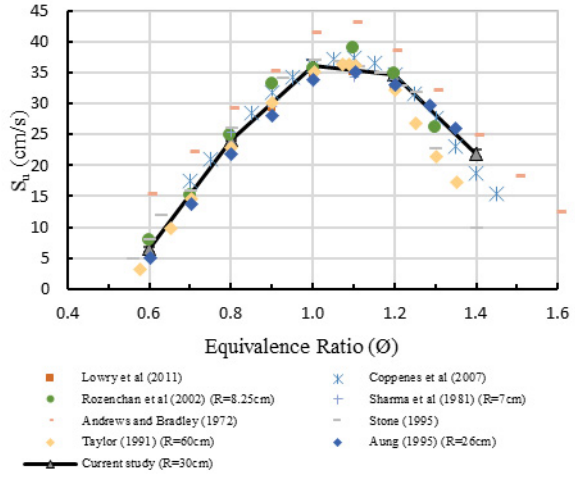

Figure 5. Comparison of experimental data for S_u of methane at standard conditions with the published results.

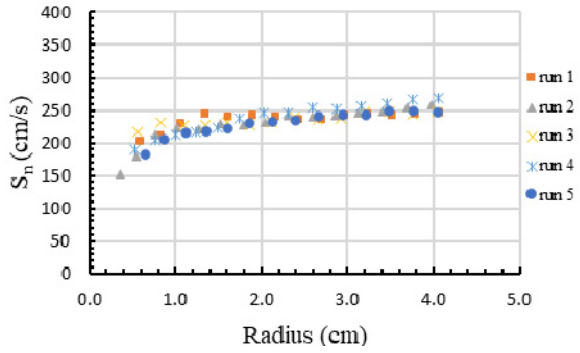

Figure 6. Stretched flame speed with flame radius for methane at T_i=306 K, P_i=1 bar, and Ø=1.

4. RESULTS AND DISCUSSIONS

In order to present an example of the flame propagation video recording, Figure (7) presents frames sequence of the spherical expanding flame for stoichiometric metha–nol/air mixture at different times and different initial temperatures. The subsequent frames are approxi–mately every 3 ms. Tracker 5.1.5 software is applied to extract information about variation of flame radius with time to follow the flame front advancement. The instantaneous stretched flame speed (S_n) is the slope of the line segment involving two neighboring radii against the time. It can be seen that the flame propagated faster when the unburned mixture temperature is higher.

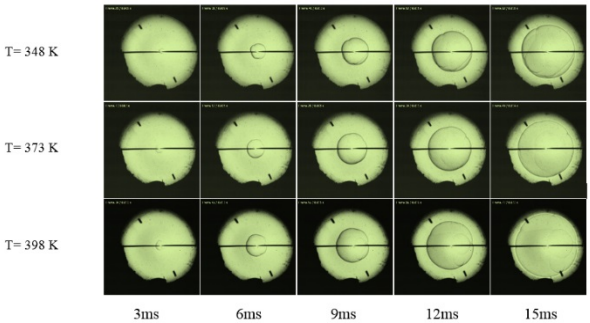

Figure 7. Photographs of flame propagation for M40 at P_0= 1.0 bar, and different initial temperatures.

4.1 Stretched laminar flame speed

The stretched laminar flame speed (S_n) has been extracted from the video recordings. Figure (8) shows the stretched laminar flame speed versus flame radius for different blending ratios and initial temperatures. The results show that the S_n increased with increasing initial temperature, since high temperatures boost the dissociation reactions that produce free radicals. These radicals initiate combustion reaction, which is why the velocity of flame propagation increased [41]. Likewise, with the increase in initial temperature, the adiabatic flame temperature increased and reaction rates become faster.

The data is extracted from the pre-pressure zone at the flame radius extending between 7-40 mm which show approximately constant flame speed with flame radius. The stretched laminar flame speed behavior subdivided into three regions. The first region; ignition affected region which is at flame radius below 7 mm, where the excess ignition energy could affect the flame propagation. Bradley et al. [42] clarified that this excess energy can overestimate the flame speed for the fuel/air mixtures at a flame radius below 5 mm. In this region the flame speed cannot be used to determine the S_u due to the interference of underdeveloped flame. The second region extends until the pressure starts to rise. In this region the stretched flame speed (S_n) would remain approximately constant. Prathap et al. [43] proposed that the flame radius smaller than one-third the radius of the combustion chamber was reasonable for the calcu–lation.

The third region begin from flame radius greater than 40 mm, where the strain in flow field would significantly change flame speed in addition to the effect of combustion pressure which is no more can be assumed constant. The first and third regions are excluded from the calculation of stretch flame speed. Sahu et al. [44] used cylindrical CC and choose 10 mm and 34mm (which forms about 4.0% of the total vessel volume) as the lower and upper critical flame radii for calculating flame speed.

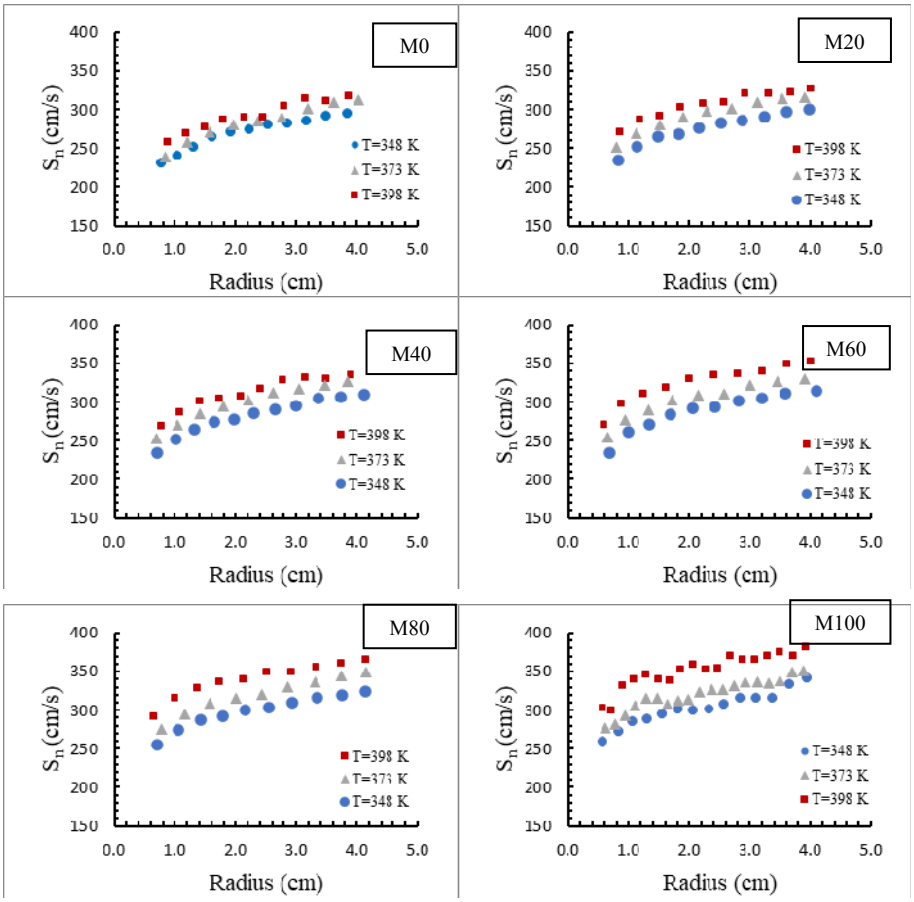

Figure 8. Variation of S_n with flame radius for different initial temperatures and blending ratios.

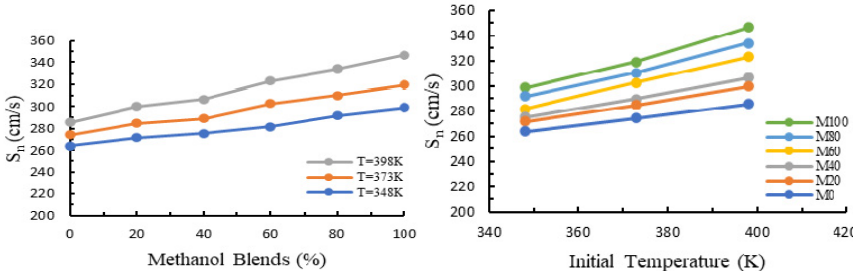

Figure 9. Variation of S_n at 20 mm flame radius versus: (a) methanol blending ratios (b) initial temperatures.

Figure (9) illustrates the variation of S_n at 20 mm flame radius with methanol blending ratio and different initial temperatures (348 K, 373 K, and 398 K). It is shown that the stretched flame speed increases with increasing methanol ratio. It is found that the value of S_n increased by about 11% for M60 at T_i=398K compared with that of pure propane (M0). It is also seen that the stretched flame speed increased with increasing initial temperatures. By rising the initial temperature for M60 from 348 K to 398 K the stretched flame speed increased by 12.8%. Similar trend is found in previous study [41]. It was also noticed that the maximum stretched flame speed has the same trend as the variation of S_n with initial temperature for all blending ratios as demonstrated in figure (10).

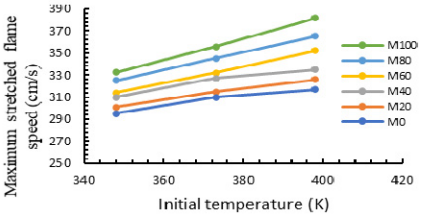

Figure 10. Variation of max. S_n versus initial temperature for different methanol blending ratios.

4.2 Un-stretched flame speed and stretched rate

When the flame-radius is small which is happened at early stage of flame propagation, the stretch rate of the flame front surface is too high due to high curvature of flame front. The stretch rate is directly proportional to the flame speed and inversely proportional with flame radius. As mentioned in the previous section the first and third region of flame propagation are excluded from the calculation and only the second region data are used to obtain the unstreched flame speed. A linear corre–lation between the flame stretch rate and the stretched flame propagation speed was used in this study.

The stretch rate is inversely proportional to the radius. Therefore, its effect decreases as the flame propagates due to the increases of flame radius. This would be expected on very general grounds since as increasing the flame radius, the flame shape becomes less curved and it seems as a planar, one-dimensional and hence, un-stretched flame. The stretch rate (α) has excessive values during the initial stages of flame propagation due to the significant curvature related with a small spherical surface. Flame speed is affected by flame stretch; it can be accurately determined when the stretch is negligible i.e. when $r \rightarrow \infty$.

The stretched flame propagation speeds decrease with the increase of stretch rate as shown in figure (11). It is clear that the influence of the stretch rate on flame during propagation is different for flames under different fuel blends and initial temperatures. It can be noticed from these graphs that the maximum stretch occurs at maximum initial temperature, and the stretched flame speeds decreased as the stretch rate increases. Similar trend was found in previous study [31]. The figure also shows that the gradients of S_n-α lines take the negative value, representing the positive values of Markstein-length.

Figure (12) presents the variation of Markstein length with initial temperature at various blending ratios. It can be noticed that Markstein length decreases with increasing both initial temperature and blending ratio. This indicates that flame stability decreased with increasing these parameters. It is clear from this figure that Markstein length of fuel blend is located between of their parent fuels.

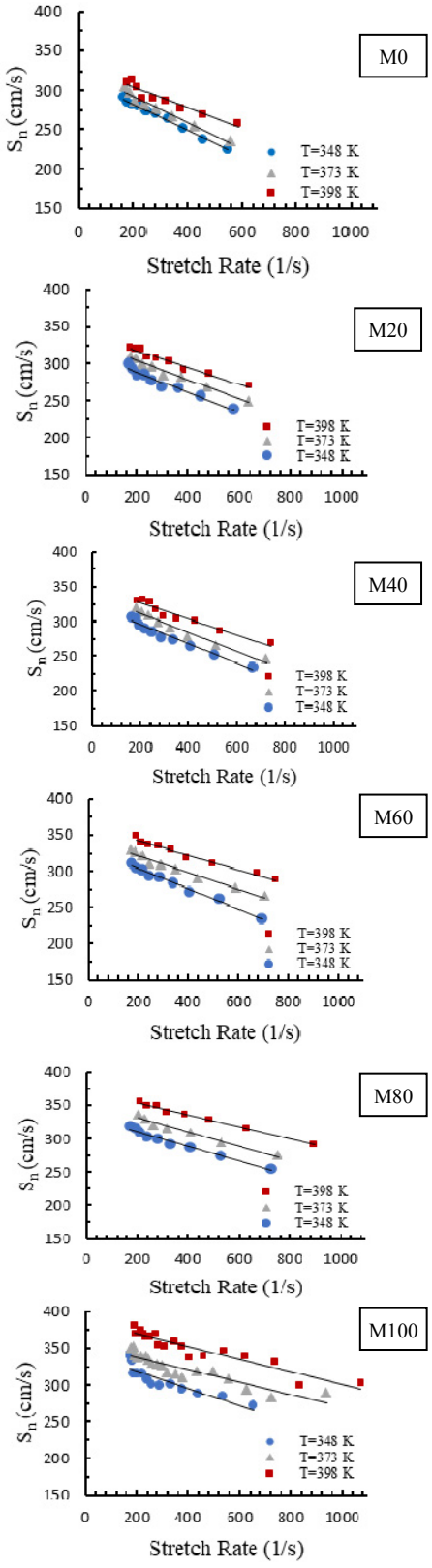

Figure 11. Stretched flame speed versus stretch rate for various initial temperatures and blending ratios

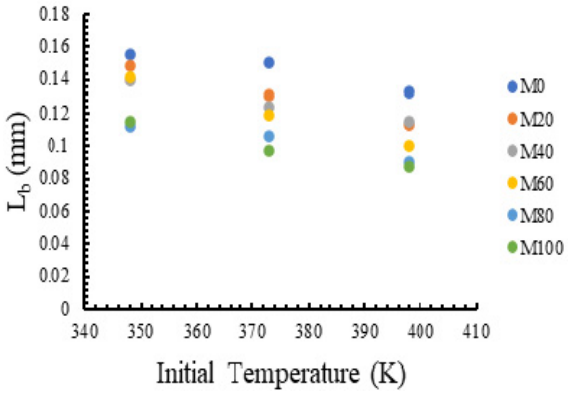

Figure 12: Markstein length versus initial temperature at different methanol blends.

The un-stretched laminar flame speed (S_l) is calcu–lated as the intercept point of S_n at α=0 in the plot of S_n versus α. The strain in the flow field causes a severe dec–rease of S_n in small stretch rate, and the cellular flame causes a severe increase of S_n in small stretch rate [21]. For reasons mentioned above the unstreched flame seed is obtained for the flame in the second stage of propagation which is at radius from 8-40 mm in the calculations.

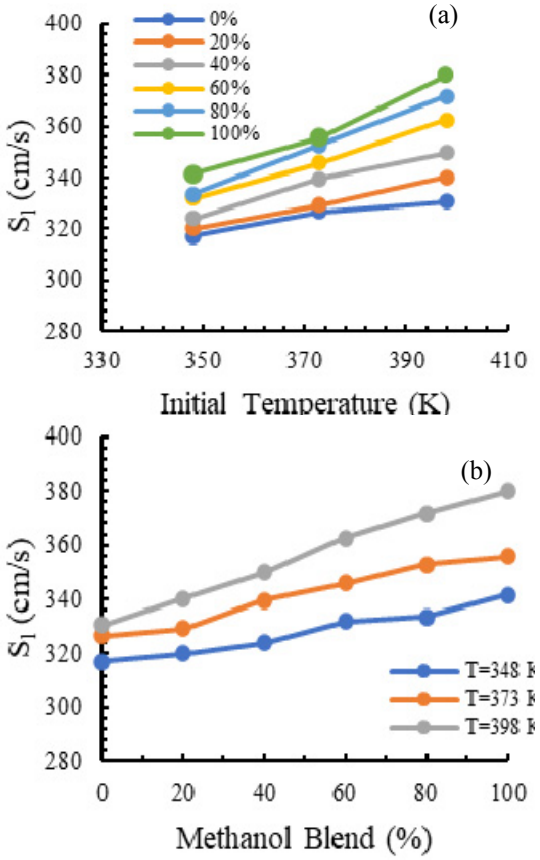

Figure 13. Unstretched flame propagation speed for stoic–hiometric mixtures versus (a) initial temperature (b) metha–nol blending ratio.

Figure (13) explains the effect initial temperature and methanol blending ratio on the unstretched flame speed (S_l). It can be seen that the unstretched flame speed increased with increasing the initial temperature. By elevating the initial temperature for M60 from 348 K to 398 K the value of the unsetreched flame speed (S_l) increased by about 8.8%. This trend is in agreement with previously published results by Bao et al. [23]. It was also noticed that S_l increased with increasing methanol blending ratio. For M60 the value of S_l at T_i=398K increased by about 9% compared with that of pure propane.

5. CONCLUSIONS

A constant volume combustion chamber has been de–sign and constracted for studying the effect of propane-methanol blending ratios, and initial temperatures on stretched and un-stretch laminar flame speed. The expe–riments are performed for the stoichiometric mixtures of different blends. The first and third stages of flame propagation are excluded from the study. High speed photography technique is used to record the flame propagation. It can be conclude from the present study that:

1- Generally, the maximum stretch rate increases with increasing the initial temperature and the blending ratio.
2- The stretched flame speed (S_n) decreases with increasing the stretch rate. Whereas, for M60 and T_i=373 K the stretch flame speed decreased from 329.6 cm/s to 265 cm/s by increasing the stretch rate from 169 s^{-1} to 702.1 s^{-1}.
3- The stretched flame speed (S_n) increased with increasing both initial temperature and methanol blending ratio. Raising the initial temperature of M60 from 348 K to 398 K led to increase the stretched flame speed by 12.8%. Furthermore, the value of S_n is increased by about 11% for M60 at T_i=398K compared with that of pure propane (M0).
4- The unstretched flame speed increased with increasing the initial temperature. By elevating the initial temperature for M60 from 348 K to 398 K the value of S_l is increased by about 8.8%.
5- The unstretched flame speed increased with increasing methanol blending ratio. For M60 the value of S_l is increased by about 9% compared with that of pure propane.
6- The Markstein length decreased with increasing both initial temperature and blending ratio. For M60 increasing the initial temperature from 348 K to 398 K reduced the Markstein length from 0.142 mm to 0.1 mm. And for T_i=373 K increasing the blending ratio from M20 to M80 reduced the Markstein length from 0.131 mm to 0.106 mm. This means that flame stability decreases with increasing these parameters. Furthermore, Markstein length of fuel blend is located between of their parent fuels.

REFERENCES

[1] Anetor, L., Osakue, E. E., Harris, K.: Simulation Studies of Combustion in Spark Ignition Engine using Openfoam, *FME Transactions*, vol. 48, no. 4, pp. 787–799, 2020.

[2] Fayad, M. A., Tsolakis, A., Fernández-Rodríguez, D., Herreros, J. M., Martos, F. J. and Lapuerta, M.: Manipulating modern diesel engine particulate emission characteristics through butanol fuel blending and fuel injection strategies for efficient diesel oxidation catalysts, Applied Energy, vol. 190, pp. 490–500, 2017.

[3] Fayad, M. A., Tsolakis, A. and Martos, F. J.: Influence of alternative fuels on combustion and characteristics of particulate matter morphology in a compression ignition diesel engine, Renewable Energy, vol. 149, pp. 962–969, 2020.

[4] Dhahad H. A. and Fayad, M. A.: Role of different antioxidants additions to renewable fuels on NOX emissions reduction and smoke number in direct injection diesel engine, Fuel, vol. 279, no. June, pp. 118384, 2020.

[5] Fayad, M. A.: Investigating the influence of oxygenated fuel on particulate size distribution and NOX control in a common-rail diesel engine at rated EGR levels, Thermal Science and Engineering Progress, vol. 19, no. June, pp. 100621, 2020.

[6] Fayad M. A. and Dhahad, H. A.: Effects of adding aluminum oxide nanoparticles to butanol-diesel blends on performance, particulate matter, and emission characteristics of diesel engine, Fuel, vol. 286, no. P2, pp. 119363, 2021.

[7] Barakat, H. Z., Kamal, M. M., Saad, H. E. and Ibrahim, B.: Blending effect between the natural gas and the liquefied petroleum gas using multiple co- and cross-flow jets on NOx emissions, Ain Shams Engineering Journal, vol. 10, no. 2, pp. 419–434, 2019.

[8] Salih, A. M. and Abass, K. I.: The Emitted Noise from a Spark Ignition Engine Fueled by Methanol Added to Gasoline, International Research Journal of Advanced Engineering and Science, vol. 3, no. 2, pp. 265–270, 2018.

[9] Zhang, Z., Huang, Z., Wang, X., Xiang, J., Wang, X. and Miao, H.: Measurements of laminar burning velocities and Markstein lengths for methanol-air-nitrogen mixtures at elevated pressures and temperatures, Combustion and Flame, vol. 155, no. 3, pp. 358–368, 2008.

[10] Zhang, Y., Li, Q., Liu, H., Yan, Z. and Huang, Z.: Comparative study on the laminar flame speeds of methylcyclohexane-methanol and toluenemetha-nol blends at elevated tempera–tures, Fuel, vol. 245, no. February, pp. 534–543, 2019.

[11] Hu, Z., Wang, Z., Guo, Y., Wang,L., Zhang, J.,and Zhan, W.: Total Oxidation of Propane over a Ru/CeO2 Catalyst at Low Temperature, *Environmental Science and Technology*, vol. 52, no. 16, pp. 9531–9541, 2018, doi: 10.1021/acs. est.8b03448.

[12] Salih, A. M. and Chaichan, M. T.: The effect of initial pressure and temperature upon the laminar burning velocity and flame stability for propane-air mixtures, Journal of Engineering, Technology and Innovation, vol. 3, no. 7, pp. 154–201, 2014.

[13] Egolfopoulos, F. N., Hansen, N., Ju, Y., Kohse-Höinghaus, K., Law, C. K. and Qi, F.: Advances and challenges in laminar flame experiments and implications for combustion chemistry, Progress in Energy and Combustion Science, vol. 43, pp. 36–67, 2014.

[14] Abdulraheem, A. A., Saleh, A. M., Shahad, H. Ak.: Measurements and Data Analysis Review of Laminar Burning Velocity and Flame Speed for Biofuel / Air Mixtures Measurements and Data Analysis Review of Laminar Burning Velocity and Flame Speed for Biofuel / Air Mixtures, in *IOP Conference Series: Materials Science and Engineering*, 2021, pp. 1-28.

[15] Chan, Y. L., Zhu, M. M., Zhang, Z. Z., Liu, P. F. and Zhang, D. K.: The Effect of CO2 Dilution on the Laminar Burning Velocity of Premixed Methane/Air Flames, Energy Procedia, vol. 75, pp. 3048–3053, 2015.

[16] Lipatnikov, A. N., Shy, S. S. and Li, W.: Experimental assessment of various methods of determination of laminar flame speed in experiments with expanding spherical flames with positive Markstein lengths, Combustion and Flame, vol. 162, no. 7, pp. 2840–2854, 2015.

[17] Salih, A. M. and Chaichan, M. T.: Study of the effect of elevated pressures on the laminar burning velocity of propane-air mixtures, in *The 2nd Scientific Conference of Engineering Science · At: Diyala, Iraq*, 2015.

[18] Galmiche, B., Halter, F., Foucher, F. and Dagaut, P.: Effects of Dilution on Laminar Burning Velocity of Premixed Methane / Air Flames, Energy & Fuels, pp. 948–954, 2011.

[19] Hinton N. and Stone, R.: Laminar burning velocity measurements of methane and carbon dioxide mixtures (biogas) over wide ranging temperatures and pressures, Fuel, vol. 116, pp. 743–750, 2014.

[20] Mannaa, O., Mansour, M. S., Roberts, W. L. and Chung, S. H.: Laminar burning velocities at elevated pressures for gasoline and gasoline surrogates associated with RON, COMBUSTION AND FLAME, 2015.

[21] Yasiry A. S. Shahad H. AK.: An experimental study of the effect of hydrogen blending on burning velocity of LPG at elevated pressure, International Journal of Hydrogen Energy, vol. 41, pp. 19269–19277, 2016.

[22] Yao, C., Hu, J., Geng, P., Shi, J., Zhang, D. and Ju, Y.: Effects of injection pressure on ignition and combustion characteristics of diesel in a premixed methanol / air mixture atmosphere in a constant volume combustion chamber, Fuel, vol. 206, pp. 593–602, 2017.

[23] Bao, X., Jiang, Y., Xu, H., Wang, C., Lattimore, T. and Tang, L.: Laminar flame characteristics of cyclopentanone at elevated temperatures, Applied Energy, vol. 195, pp. 671–680, 2017.

[24] Lhuillier, C., Brequigny, P., Lamoureux, N., Contino, F. and Mounaïmrousselle, C.: Experimental investigation on laminar burning velocities of ammonia/hydrogen / air mixtures at elevated temperatures, Fuel, no. November, p. 116653, 2019.

[25] Linteris, G. and Babushok, V.: Laminar Burning Velocity Predictions for C1 and C2 Hydrofluorocarbon Refrigerants with Air, Journal of Fluorine Chemistry, 2019.

[26] Duva, B. C., Chance, L. E. and Toulson, E.: Dilution e ff ect of di ff erent combustion residuals on laminar burning velocities and burned gas Markstein lengths of premixed methane / air mixtures at elevated temperature, Fuel, vol. 267, no. December 2019.

[27] Konnov, A. A., Mohammad A., Kishore V. R. Chockalingam S. K., A comprehensive review of measurements and data analysis of laminar burning velocities for various fuel + air mixtures Mohammad D9X b, Progress in Energy and Combustion Science, vol. 68, pp. 197–267, 2018.

[28] Varghese, R. J. and Kumar, S.: Machine learning model to predict the laminar burning velocities of H 2 / CO / CH 4 / CO 2 / N 2 / air mixtures at high pressure and temperature conditions, International Journal of Hydrogen Energy, 2019.

[29] Han, Z., Zhu, Z., Wang, P., Liang, K., Zuo, Z. and Zeng, D.: energies The Effect of Initial Conditions on the Laminar, Energies, vol. 12, p. 2892, 2019.

[30] Metghalchi, M. and Keck, J. C.: Burning velocities of mixtures of air with methanol, isooctane, and indolene at high pressure and temperature, Combustion and Flame, vol. 48, no. C, pp. 191–210, 1982.

[31] Beeckmann, J., Röhl, O. and Peters, N.: Experimental and numerical investigation of iso-octane, methanol and ethanol regarding laminar burning velocity at elevated pressure and temperature, *SAE Technical Papers*, vol. 4970, 2009.

[32] Li, Q., Zhang, W., Jin, W., Xie, Y. and Huang, Z.: Laminar flame characteristics and kinetic modeling study of methanol-isooctane blends at elevated temperatures, Fuel, vol. 184, pp. 836–845, 2016.

[33] Liu, X., Ji, C., Gao, B., Wang, S., Liang, C. and Yang, J.: A laminar flame speed correlation of hydrogen-methanol blends valid at engine-like conditions, International Journal of Hydrogen Energy, vol. 38, no. 35, pp. 15500–15509, 2013.

[34] Andrews, G. E. and Bradley, D.: Determination of burning velocities: A critical review, Combustion and Flame, vol. 18, no. 1, pp. 133–153, 1972.

[35] Sharma, C. P. G. S.P. and Agrawal, D.D.: The pressure and temperature dependence of burning velocity in a spherical combustion bomb, Proc. Combust. Inst., vol. 18, pp. 493–501, 1981.

[36] Rozenchan, G., Zhu, D. L., Law, C. K. Tse, S. D.: Outward propagation, burning velocities, and chemical effects of methane flames up to 60 ATM, Proceedings of the Combustion Institute, vol. 29, no. 2, pp. 1461–1470, 2002.

[37] Lowry, E. P. W., Vries, J. de, Krejci, M.: Laminar flame speed measurements and modeling of pure alkanes and alkane blends at elevated pressures, J. Eng. Gas Turbines Power, vol. 133, p. 091501, 2011.

[38] Clarke, P., Stone, A., Beckwith, R.: Measuring the laminar burning velocity of methane/diluent/air mixtures within a constant-volume combustion bomb in a micro-gravity environment, J. Inst. Energy, vol. 68, p. 130, 1995.

[39] Taylor, S. C.: Burning velocity and the influ–ence of flame stretch. Ph.D. Thesis, University of Leeds, 1991.

[40] Aung, K. T., Tseng, L. K., Ismail, M. A. and Faeth, G. M.: Response to comment by S.C. Taylor and D.B. Smith on 'laminar burning velocities and Markstein numbers of hydrocarbon/air flames, Combustion and Flame, vol. 102, no. 4, pp. 526–530, 1995.

[41] Baloo, M., Dariani, B. M., Akhlaghi, M. and Aghamirsalim, M.: Effects of pressure and temperature on laminar burning velocity and flame instability of iso-octane/methane fuel blend, Fuel, vol. 170, no. 424, pp. 235–244, 2016.

[42] Bradley, D., Hicks, R. A., Lawes, M., Sheppard, C. G. W., and Woolley, R.: The measurement of laminar burning velocities and Markstein numbers for isooctane-air and isooctane-n-heptane-air mixtures at elevated temperatures and pressures in an explosion bomb, Combustion and Flame, vol. 115, pp. 126–144, 1998.

[43] Prathap, C., Ray, A. Ravi, M. R.: Investigation of nitrogen dilution effects on the laminar burning velocity and flame stability of syngas fuel at atmospheric condition, Combustion and Flame, vol. 155, no. 1–2, pp. 145–160, 2008.

[44] Sahu, A., Wang, C., Jiang, C., Xu, H., Ma, X., Xu, C. and Bao, X.: Effect of CO2 and N2 dilution on laminar premixed MTHF/air flames: Experiments and kinetic studies, Fuel, vol. 255, no. June, 2019.

УТИЦАЈ ОДНОСА МЕШАЊА ПРОПАНА И МЕТАНОЛА НА БРЗИНЕ РАСТЕГНУТОГ И НЕРАСТЕГНУТОГ ПЛАМЕНА НА ПОВИШЕНИМ ПОЧЕТНИМ ТЕМПЕРАТУРАМА

А.А. Абдулрахим, А.М. Салех, А.К. Шахад

Брзина нерастегнутог пламена мешавине пропан-метанол/ваздух је експериментално проучавана у комори за сагоревање константне запремине са централним паљењем. Експерименти су рађени при атмосферском притиску и стехиометријском односу ваздух/гориво. У овом истраживању коришћени су различити односи мешања метанола (0%, 20%, 40%,

60%, 80%, 100%) и различите повишене почетне температуре (348 К, 373 К и 398 К). Уопштено говорећи, резултати су показали да се брзина нерас–тегнутог пламена повећава са повећањем и односа мешања метанола и почетне температуре. За М60 вредност повећања брзине пламена при T_i = 398К била је око 9% у поређењу са чистом про–паном, а повећањем почетне температуре за исти однос мешавине (М60) са 348 К на 398 К вредност прираста је била око 8,8%. Такође је примећено да се Маркштајнова дужина смањује са повећањем и почетне температуре и односа мешања, што указује да се нестабилност пламена повећава са повећањем ових параметара.